

ChemComm

Chemical Communications

Accepted Manuscript

This article can be cited before page numbers have been issued, to do this please use: W. Ma, X. Song, J. Yin and H. Fei, *Chem. Commun.*, 2021, DOI: 10.1039/D0CC07320B.



This is an Accepted Manuscript, which has been through the Royal Society of Chemistry peer review process and has been accepted for publication.

Accepted Manuscripts are published online shortly after acceptance, before technical editing, formatting and proof reading. Using this free service, authors can make their results available to the community, in citable form, before we publish the edited article. We will replace this Accepted Manuscript with the edited and formatted Advance Article as soon as it is available.

You can find more information about Accepted Manuscripts in the [Information for Authors](#).

Please note that technical editing may introduce minor changes to the text and/or graphics, which may alter content. The journal's standard [Terms & Conditions](#) and the [Ethical guidelines](#) still apply. In no event shall the Royal Society of Chemistry be held responsible for any errors or omissions in this Accepted Manuscript or any consequences arising from the use of any information it contains.

COMMUNICATION

Intrinsic Self-Trapped Broadband Emission from Zinc Halide-Based Metal-Organic FrameworksReceived 00th January 20xx,
Accepted 00th January 20xxWen Ma,^a Xueling Song,^a Jinlin Yin,^a and Honghan Fei^{a,*}

DOI: 10.1039/x0xx00000x

Organolead halide perovskites are an emerging class of intrinsic self-trapped broadband emitters, but suffer from lead toxicity and stability problems. Herein, we report a series of metal-organic frameworks (MOFs) based on 0-D zinc halide secondary building units (SBUs), which emit large Stokes shifted broadband bluish-white light. A variety of photophysics studies demonstrate the broadband emission probably originate from self-trapped excitons, owing to the structurally deformable SBUs. Among the intrinsic self-trapped emitters, these MOFs are very rare examples to occupy both long-term environmental stability and non-toxic elements. Moreover, the open porosity serve the MOF as a host matrix for encapsulating green-emitting Alq3 molecules, exhibiting cold white-light chromatic coordinates of (0.27,0.36) and correlated color temperature of 8321 K.

White light-emitting diodes (WLEDs), the next-generation candidate in solid-state lighting technology, have attracted great attentions owing to their high energy-efficiency and long-term stability.^{1,2} The conventional approach to assemble WLEDs is combining blue InGaN LEDs and yellow-emitting phosphors (e.g. $\text{Y}_3\text{Al}_5\text{O}_{12}:\text{Ce}^{3+}$), which suffer a variety of drawbacks including self-absorption and colour aging.^{3,4} Thus, it is highly desirable to develop an UV-excited single-component broadband white-light emitting phosphor.^{5,6}

Recently, organolead halide perovskites are an emerging class of intrinsic broadband white-light phosphors, resulting from self-trapped excitons in the deformable lattice.⁷⁻¹⁰ Lowering the inorganic dimensionality to 0-D is an effective strategy to enhance the photoluminescence quantum efficiency (PLQE), owing to the strong exciton confinement and populated self-trapped states. However, the hydrophilic nature of organoammonium cations in many perovskites affords them to be susceptible to hydrolysis even under ambient conditions. Our group have employed anionic organocarboxylates (instead of organoammonium cations) to template a class of cationic

lead halide frameworks, demonstrating robustness over a wide range of pH as well as aqueous boiling condition.¹¹⁻¹⁵ However, the lead toxicity problem must be solved for WLED applications. It is highly important to construct lead-free, water-stable metal halide materials.¹⁶⁻¹⁹

Metal-organic frameworks (MOFs) incorporating multiple luminescent centers is a promising platform to achieve white-light emission.²⁰⁻²² The porosity of open frameworks allows for precise tuning of luminescence by introduction of guest-based emission center.²² So far, the vast majority of white-light-emissive MOFs are based on emissions from several rare-earth metal ions (e.g. Ln^{3+}) despite the self-absorption problems as well as overwhelming demands for rare earth elements.^{23,24} Broadband white-light emission from non-rare-earth MOFs often arise from ligand-based photoluminescence (PL) and/or charge transfer between metal nodes and linkers (MLCT/LMCT).²⁴⁻²⁶ Very few MOFs exhibit broadband white-light emission originating only from the inorganic building blocks, until our very recent findings in $\text{Pb}^{2+}/\text{Cd}^{2+}$ halide-based MOFs with structurally deformable secondary building units (SBUs).^{12,15,27} In contrast to lead perovskites, this class of single-source, broadband white-light emitters have many intriguing attributes including introduction of guest molecules and facile functionalization of photoactive species.

Herein, we have studied the intrinsic broadband emission from a series of Zn^{2+} -based MOFs based on $[\text{Zn}_5\text{X}_4]^{6+}$ ($\text{X}=\text{Cl}/\text{Br}/\text{I}$) as SBUs and bis(1H-1,2,3-triazolo[4,5-b],[4',5'-i])dibenzo[1,4]dioxin (H_2BTDD) as organic linkers. A variety of variable-temperature photophysics studies indicate the large Stokes shifted emission probably originate from self-trapped excitons. Moreover, the green-emitting tris(8-hydroxyquinoline) aluminium(III) (Alq3) molecules have been successfully incorporated into the MOF porosity, achieving cold white-light emission with Commission Internationale de l'Eclairage (CIE) chromatic coordinates of (0.27, 0.36) and correlated colour temperature (CCT) of 8321 K.

$\text{Zn}_5\text{Cl}_4\text{BTDD}_3(\text{MFU}-4\text{l}(\text{Zn})-\text{Cl})$, consisting of 6-connected $[\text{Zn}_5\text{Cl}_4]^{6+}$ nodes and BTDD^{2-} struts, was chosen because of its high chemical stability and non-toxic metal (Fig. 1a and b). $\text{MFU}-4\text{l}(\text{Zn})-\text{Cl}$ was synthesized under solvothermal conditions

Shanghai Key Laboratory of Chemical Assessment and Sustainability, School of Chemical Science and Engineering, Tongji University, 1239 Siping Rd., Shanghai 200092, P. R. China. E-mail: fei@tongji.edu.cn
†Electronic supplementary information (ESI) available: Experimental details and additional characterization. See DOI: 10.1039/x0xx00000x

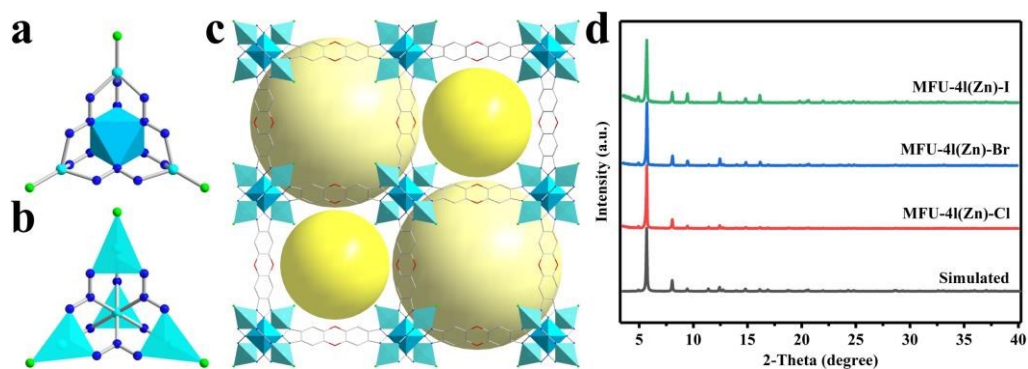


Fig. 1 (a,b) Crystallographic view of two crystallographic independent Zn^{2+} in $[\text{Zn}_5\text{Cl}_4]^{6+}$ nodes, octahedral coordinated Zn^{2+} (blue) (a) and tetrahedral coordinated Zn^{2+} (turquoise) (b); (c) crystallographic view of MFU-4l(Zn)-Cl along the a-axis; (d) simulated X-ray diffraction (XRD) pattern of MFU-4l(Zn)-Cl and powder X-ray diffraction (PXRD) patterns of synthesized MFU-4l(Zn)-X (X = Cl, Br, I). Zn turquoise, Cl green, N blue, O red, C grey, yellow spheres represent the void inside the cages. Hydrogen atoms are omitted for clarity.

using anhydrous ZnCl_2 and H_2BTDD in DMF at 145 °C, according to the previous literature.²⁸

The resultant material has no N-H stretching vibration ($\sim 3200\text{ cm}^{-1}$) in fourier-transform infrared spectroscopy (FTIR), suggesting the complete conversion of H_2BTDD (Fig. S2, ESI†). Activated MFU-4l(Zn)-Cl exhibits a characteristic type-I sorption behaviour, corresponding to the microporous nature. The Brunauer-Emmett-Teller (BET) surface area is calculated to be $3096.55\text{ cm}^3/\text{g}$, measured with N_2 sorption isotherm at 77 K (Fig. S4, ESI†).

Importantly, the isoreticular synthesis of the bromide and iodide analogs were successful when using ZnBr_2 or ZnI_2 in place of ZnCl_2 during solvothermal synthesis. Both PXRD and elemental analysis evidence the high phase purity of MFU-4l(Zn)-Br and MFU-4l(Zn)-I (Fig. 1d and experimental Section in ESI†). Indeed, all three materials show well-defined cubic microcrystalline morphology by scanning electron microscopy (SEM) (Fig. S3, ESI†). A reasonable decrease of BET surface area from $3096.55\text{ cm}^3/\text{g}$ (MFU-4l(Zn)-Cl) to $2669.95\text{ cm}^3/\text{g}$ (MFU-4l(Zn)-Br) and $2259.68\text{ cm}^3/\text{g}$ (MFU-4l(Zn)-I) was observed (Fig. S4, ESI†). The as-synthesized MFU-4l(Zn)-X (X=Cl/Br/I) demonstrate high chemical stability in both aqueous condition and common organic solvents (e.g. EtOH, DCM, and DMF). No significant loss in both crystallinity decrease and mass balance after incubating the MOFs in these solvents for 24 h (Fig. S5, ESI†). The important moisture stability overcomes the hydrolysis problems in organolead halide perovskites. Thermogravimetric analysis (TGA) and *ex-situ* thermodiffraction again indicate the high thermal stability of MFU-4l(Zn) up to 350 °C (Fig. S6 and S7, ESI†).

Valence band maximum (VBM) of three materials were measured to be 2.98 eV for MFU-4l(Zn)-Cl, 2.28 eV for the bromide analog and 1.98 eV for the iodide analog, respectively, by linearly extrapolating the low-binding-energy edge of X-ray photoelectron spectroscopy (Fig. S8, ESI†). The halide-dependent VBM is consistent with the trend of organolead halide perovskites. However, UV-vis absorption spectroscopy show analogous band gap of 3.39 eV (366 nm) for MFU-4l(Zn)-Cl, 3.62 eV (364 nm) for MFU-4l(Zn)-Br and 3.43 eV (362 nm) for MFU-4l(Zn)-I, respectively, presumably owing to the absorption from the conjugated triazolate-based ligand (Fig. S9 and S10, ESI†). Upon 365 nm excitation at room temperature, both as-synthesized MFU-4l(Zn)-Cl and MFU-4l(Zn)-Br exhibit broadband bluish white-light with emission centered at 467 and 466 nm, respectively (Fig. 2a and b). Although the large Stokes shifts of $\sim 100\text{ nm}$ is slightly lower than emission from organolead halide materials, these values are often the cases in self-trapped emission from d^{10} metal-based perovskites.^{29, 30} The iodide analog shows a

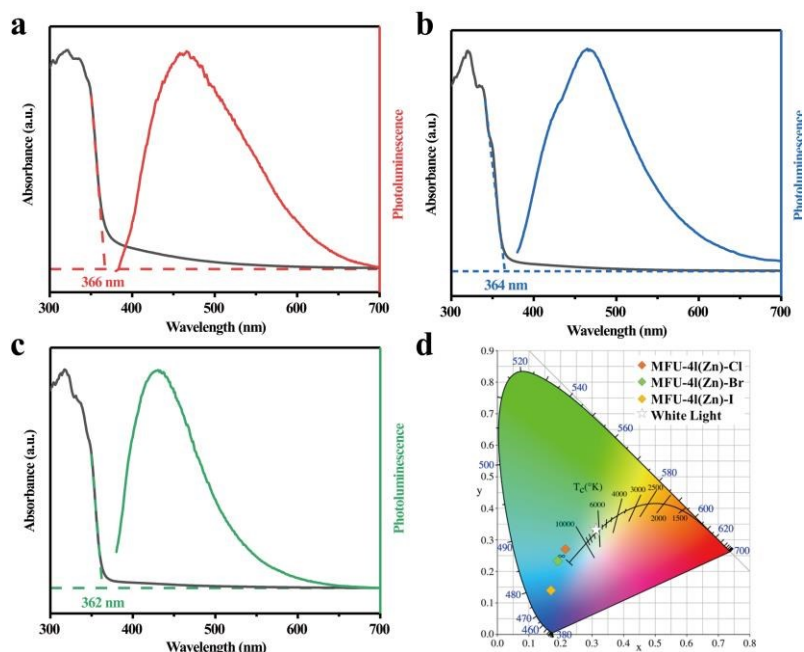


Fig. 2 Absorption (black) and room temperature emission spectra of MFU-4l(Zn)-Cl (a, red), MFU-4l(Zn)-Br (b, blue) and MFU-4l(Zn)-I (c, green); (d) CIE chromaticity coordinates of MFU-4l(Zn).

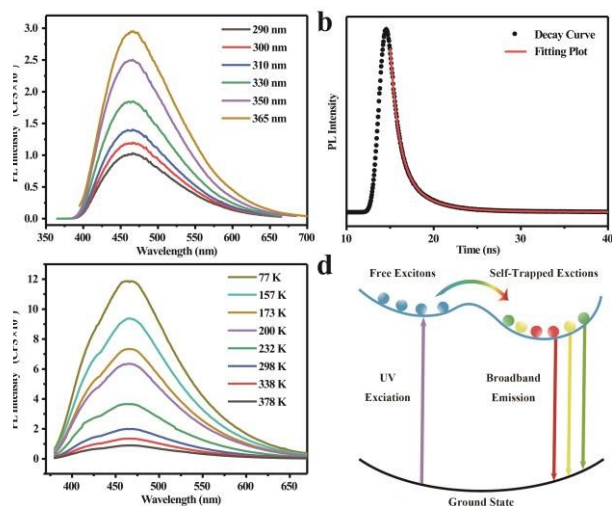


Fig. 3 (a,b) Excitation-dependent (a) and temperature-dependent (b) emission spectra of MFU-4l(Zn)-Br; (c) photoluminescence decay of MFU-4l(Zn)-Br at room temperature (monitored at 340 nm); (d) configuration coordinate diagram for the structural-deformation-induced large Stokes-shift broadband emission.

sharper emission centered at 433 nm probably owing to the weaker structural deformation, which has been commonly observed in lead iodide perovskites (Fig. 2c).^{8, 31} Importantly, H₂BTDD ligand shows a different emission with two PL maxima at 390 and 510 nm, resulting from the n- π^* electronic transitions in triazolate ligands (Fig. S11, ESI[†]). This study suggests the broadband emission of MFU-4l(Zn) originate from metal-halide SBUs.

The photoemission afford Commission Internationale de l'Éclairage (CIE) chromatic coordinates of (0.22,0.27) for MFU-4l(Zn)-Cl, (0.19,0.23) for MFU-4l(Zn)-Br, and (0.17,0.14) for MFU-4l(Zn)-I, respectively, corresponding to the so-called “cold” white-light emission (Fig. 2d and Fig. S12, ESI[†]). The highest external PLQE of the three materials reaches 3.2% for the bromide analog, while the chloride and iodide have PLQE of ~1% (Table S1, ESI[†]). Notably, all of the three MFU-4l(Zn) exhibit stable PL upon continuous irradiation (365 nm, 4 W) under ambient condition for up to 7 days (Fig. S13, ESI[†]). Moreover, no obvious change in both PL intensity and broadening of the emission have been noticed after chemical treatment in different solvents (*e.g.* DMF, H₂O and EtOH) for 24 h and thermal treatment in air up to 350 °C (Fig. S14~S16, ESI[†]).

Given the high robustness and broadband emission of MFU-4l(Zn), we continue to investigate the PL mechanism. First, no obvious change was observed from the excitation-dependent PL from 290 nm to 365 nm excitation, agreeing with the claim of intrinsic self-trapped emission (Fig. 3a). Moreover, the time-resolved photoluminescence decay study indicates a short PL lifetime of 2.34 ns for MFU-4l(Zn)-Br, which resides well in the range of self-trapped excitons (Fig. 3b).³² The temperature-dependent PL study demonstrates sharper emission and higher intensity when temperature decreasing from 378 to

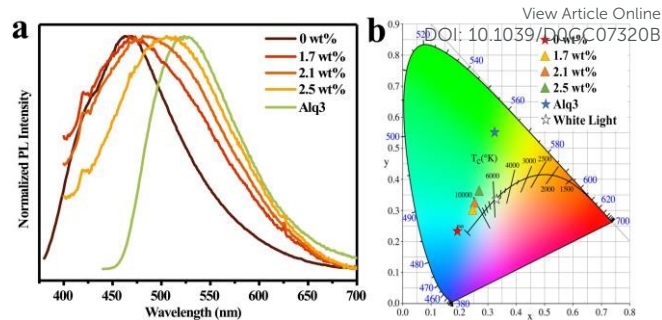


Fig. 4 (a) Normalized emission spectra of different degree of functionalized Alq3@MFU-4l(Zn)-Br; (b) CIE chromaticity coordinates of different degree of functionalized Alq3@MFU-4l(Zn)-Br. PL measurements were performed upon 365 nm excitation.

77 K (Fig. 3c), which evidences the self-trapped emission arising from strong electron-phonon coupling. The presence of 0-D inorganic building units with high structural strain often contain strongly localized excitons, which further induce highly distorted sub-lattice and strong electron-phonon coupling.^{10, 33, 34} Assuming the harmonic lattice vibration, the phonon energy can be estimated from the temperature-dependent FWHM by following equation:^{7,8,35}

$$\Gamma(T) = \Gamma_0 + \Gamma_{LO} (e^{E_{LO}/k_B T} - 1)^{-1} + \Gamma_{inh} e^{-E_b/k_B T} \quad (1)$$

where Γ_0 is the FWHM of the broadband emission when $T = 0$ K, Γ_{LO} and Γ_{inh} represent the contribution of electron-phonon coupling and inhomogeneous broadening of the FWHM. The best fit (see fitting details in Fig. S17, ESI[†]) indicates Γ_{LO} of 126(7) meV and phonon energy (E_{LO}) of 25(3) meV, corresponding to the Raman-active Zn-Br frequency of 212 cm^{-1} (Fig. S18, ESI[†]). Thus, these advanced photophysics studies indicate the broadband emission probably originate from self-trapped excitons (*e.g.* dimerized Zn_2^{3+} species, Zn^{2+} - Zn^{2+} distance of 3.64 Å) in deformable SBUs.

In order to achieve white-light emission, we sought to investigate the incorporation of luminescence guest molecules into the MOF porosity. Since MFU-4l(Zn)-Br occupying two different pore cages with ~15 Å and 12 Å in diameter, Alq3 complexes with efficient green emission and suitable molecule size (9 Å) were chosen to be encapsulated in the MOF. Treatment of Alq3 was performed by introducing 10 mg MFU-4l(Zn)-Br into a 10 mL DMF solution containing 1 mg Alq3. After incubating the mixture at room temperature for a certain period of time (*i.e.* 0.5, 1.5 and 3 h), the Alq3 degree of functionalization reaches 1.7 wt%, 2.1 wt% and 2.5 wt%, respectively (Table S2, ESI[†]). PXRD patterns and FTIR spectra indicate the post-functionalized MOFs retain the parent framework (Fig. S19 and S20, ESI[†]). SEM images reveal Alq3@MFU-4l(Zn)-Br retaining the cubic microcrystalline morphology after Alq3 treatment (Fig. S21, ESI[†]). Energy-dispersive X-ray spectroscopy (EDS) elemental mapping confirm the homogeneous distribution of Alq3 molecules in the porosity of MFU-4l(Zn)-Br (Fig. S22, ESI[†]). Meanwhile, N₂ absorption isotherm suggest a moderate decrease of BET surface area from 2669.95 cm^3/g (MFU-4l(Zn)-Br) to 2250.86

cm³/g (2.5% Alq3@MFU-4l(Zn)-Br), suggesting the successful encapsulation of Alq3 in the porosity of MFU-4l(Zn)-Br (Fig. S23 and S24, ESI†). Upon 365 nm UV irradiation, the MOFs exhibit tunable white-light emission with CIE coordinates from (0.19, 0.23) for MFU-4l(Zn)-Br to (0.27, 0.36) for 2.5% Alq3@MFU-4l(Zn)-Br (Fig. 4 and Fig. S25, ESI†). The latter is close to (0.33, 0.33) of the pure white light, corresponding to CCT of 8321 K. PL excitation of Alq3 is centered at 462 nm and resides well in the broadband emission of MFU-4l(Zn)-Br, suggesting the electron transfer process between Alq3 and MFU-4l(Zn)-Br (Fig. S26, ESI†). Again, the process is further confirmed by the longer PL lifetime of MFU-4l(Zn)-Br with encapsulated Alq3 increasing from 1.7 wt% to 2.5 wt% (Table S2 and Fig. S27, ESI†).

In conclusion, we report three new members of intrinsic broadband light-emissive MOFs based on 0-D [Zn₅X₄]⁶⁺ (X=Cl/Br/I) SBUs, overcoming the lead toxicity problems in many lead halide-based white-light phosphors. In addition, the chemical robust nature of MFU-4l(Zn) achieves undiminished photoemission upon continuous UV irradiation under ambient condition (~60% RH). The open porosity of MFU-4l(Zn) provide an excellent platform to encapsulate Alq3 as a second emission center to further tune the PL. We believe this study significantly advances the advantages of MOFs (e.g. porosity, stability and non-toxic metal) into the field of lead halide self-trapped white-light emitters.

This work was supported by grants from the National Natural Science Foundation of China (21971197 and 51772217), the Shanghai Rising-Star Program (No.20QA1409500), the Recruitment of Global Youth Experts by China and the Science & Technology Commission of Shanghai Municipality (19DZ2271500).

Conflicts of interest

There are no conflicts to declare.

Notes and references

- E. F. Schubert and J. K. Kim, *Science*, 2005, **308**, 1274-1278.
- S. Pimpitkar, J. S. Speck, S. P. DenBaars and S. Nakamura, *Nat. Photonics*, 2009, **3**, 180-182.
- S. Nakamura, *Angew. Chem., Int. Ed.*, 2015, **54**, 7770-7788.
- M. Shang, C. Li and J. Lin, *Chem. Soc. Rev.*, 2014, **43**, 1372-1386.
- Y. W. Zhao, F. Q. Zhang and X. M. Zhang, *ACS Appl. Mater. Interfaces*, 2016, **8**, 24123-24130.
- L. Wang, W. Li, L. Yin, Y. Liu, H. Guo, J. Lai, Y. Han, G. Li, M. Li, J. Zhang, R. Vajtai, P. M. Ajayan and M. Wu, *Sci. Adv.*, 2020, **6**, eabb6772.
- E. R. Dohner, E. T. Hoke and H. I. Karunadasa, *J. Am. Chem. Soc.*, 2014, **136**, 1718-1721.
- E. R. Dohner, A. Jaffe, L. R. Bradshaw and H. I. Karunadasa, *J. Am. Chem. Soc.*, 2014, **136**, 13154-13157.
- J. Li, J. Wang, J. Ma, H. Shen, L. Li, X. Duan and D. Li, *Nat. Commun.*, 2019, **10**, 806.
- Z. Yuan, C. Zhou, Y. Tian, Y. Shu, J. Messier, J. C. Wang, L. J. van de Burgt, K. Kountouriotis, Y. Xin, E. Holt, K. Schanze, R. Clark, T. Siegrist and B. Ma, *Nat. Commun.*, 2017, **8**, 14051.
- Z. Zhuang, C. Peng, G. Zhang, H. Yang, J. Yin and H. Fei, *Angew. Chem., Int. Ed.*, 2017, **56**, 14411-14416.
- C. Peng, Z. Zhuang, H. Yang, G. Zhang and H. Fei, *Chem. Sci.*, 2018, **9**, 1627-1633.
- J. Yin, H. Yang and H. Fei, *Chem. Mater.*, 2019, **31**, 3909-3916.
- C. Peng, X. Song, J. Yin, G. Zhang and H. Fei, *Angew. Chem., Int. Ed.*, 2019, **58**, 7818-7822.
- X. Song, C. Peng, X. Xu, J. Yin and H. Fei, *Chem. Commun.*, 2020, **56**, 10078-10081.
- L. Zhou, J. F. Liao, Z. G. Huang, X. D. Wang, H. Y. Chen and D. B. Kuang, *Angew. Chem., Int. Ed.*, 2019, DOI: 10.1002/anie.201907503.
- L. J. Xu, H. Lin, S. Lee, C. Zhou, M. Worku, M. Chaaban, Q. He, A. Plaviak, X. Lin, B. Chen, M.-H. Du and B. Ma, *Chem. Mater.*, 2020, **32**, 4692-4698.
- I. Spanopoulos, I. Hadar, W. Ke, P. Guo, S. Sidhik, M. Kepenekian, J. Even, A. D. Mohite, R. D. Schaller and M. G. Kanatzidis, *J. Am. Chem. Soc.*, 2020, **142**, 9028-9038.
- Y. Liu, Y. Jing, J. Zhao, Q. Liu and Z. Xia, *Chem. Mater.*, 2019, **31**, 3333-3339.
- Y. Cui, Y. Yue, G. Qian and B. Chen, *Chem. Rev.*, 2012, **112**, 1126-1162.
- M. D. Allendorf, C. A. Bauer, R. K. Bhakta and R. J. T. Houk, *Chem. Soc. Rev.*, 2009, **38**, 1330-1352.
- C. Y. Sun, X. L. Wang, X. Zhang, C. Qin, P. Li, Z. M. Su, D. X. Zhu, G. G. Shan, K. Z. Shao, H. Wu and J. Li, *Nat. Commun.*, 2013, **4**, 2717.
- T. Mondal, S. Mondal, S. Bose, D. Sengupta, U. K. Ghorai and S. K. Saha, *J. Mater. Chem. C*, 2018, **6**, 614-621.
- Y. Cui, B. Chen and G. Qian, *Coordin. Chem. Rev.*, 2014, **273-274**, 76-86.
- M. S. Wang, S. P. Guo, Y. Li, L. Z. Cai, J. P. Zou, G. Xu, W. W. Zhou, F. K. Zheng and G. C. Guo, *J. Am. Chem. Soc.*, 2009, **131**, 13572-13573.
- D. F. Sava, L. E. Rohwer, M. A. Rodriguez and T. M. Nenoff, *J. Am. Chem. Soc.*, 2012, **134**, 3983-3986.
- G. Zhang, J. Yin, X. Song and H. Fei, *Chem. Commun.*, 2020, **56**, 1325-1328.
- D. Denysenko, M. Grzywa, M. Tonigold, B. Streppel, I. Krkljus, M. Hirscher, E. Mugnaioli, U. Kolb, J. Hanss and D. Volkmer, *Chem. Eur. J.*, 2011, **17**, 1837-1848.
- T. D. Creason, T. M. McWhorter, Z. Bell, M. H. Du and B. Saparov, *Chem. Mater.*, 2020, **32**, 6197-6205.
- C. Sun, Y. H. Guo, Y. Yuan, W. X. Chu, W. L. He, H. X. Che, Z. H. Jing, C. Y. Yue and X. W. Lei, *Inorg. Chem.*, 2020, **59**, 4311-4319.
- D. Cortecchia, S. Neutzner, A. R. Srimath Kandada, E. Mosconi, D. Meggiolaro, F. De Angelis, C. Soci and A. Petrozza, *J. Am. Chem. Soc.*, 2017, **139**, 39-42.
- A. Yangui, R. Rocanova, T. M. McWhorter, Y. Wu, M. H. Du and B. Saparov, *Chem. Mater.*, 2019, **31**, 2983-2991.
- L. Mao, P. Guo, M. Kepenekian, I. Hadar, C. Katan, J. Even, R. D. Schaller, C. C. Stoumpos and M. G. Kanatzidis, *J. Am. Chem. Soc.*, 2018, **140**, 13078-13088.
- C. Zhou, H. Lin, Y. Tian, Z. Yuan, R. Clark, B. Chen, L. J. van de Burgt, J. C. Wang, Y. Zhou, K. Hanson, Q. J. Meisner, J. Neu, T. Besara, T. Siegrist, E. Lambers, P. Djurovich and B. Ma, *Chem. Sci.*, 2018, **9**, 586-593.
- J. Lee, E. S. Koteles and M. O. Vassell, *Phys. Rev. B*, 1986, **33**, 5512-5516.

Table of Content

View Article Online
DOI: 10.1039/D0CC07320B

MFU-4l(Zn) are a class of non-toxic metal-based intrinsic self-trapped broadband emitters, which have high stability and can be functionalized by luminescent Alq3 guests.

